Journal of Alloys and Compounds 712 (2017) 687–695

Contents lists available at ScienceDirect

Journal of Alloys and Compounds

journal homepage: http://www.elsevier.com/locate/jalcom

Deformation behavior and processing maps of Ni_3Al-based superalloy during isothermal hot compression

Yuting Wu [a], Yongchang Liu [a, *], Chong Li [a, **], Xingchuan Xia [a], Yuan Huang [a], Huijun Li [a], Haipeng Wang [b]

[a] State Key Lab of Hydraulic Engineering Simulation and Safety, School of Materials Science & Engineering, Tianjin University, Tianjin 300354, PR China
[b] Department of Applied Physics, School of Science, Northwestern Polytechnical University, Xi'an 710129, PR China

ARTICLE INFO

Article history:
Received 7 January 2017
Received in revised form
6 April 2017
Accepted 12 April 2017
Available online 13 April 2017

Keywords:
Ni_3Al-based alloy
Hot deformation behavior
Constitutive equation
Processing map
Dynamic recrystallization

ABSTRACT

To study the hot deformation behavior of Ni_3Al-based alloy, hot compression tests were conducted in the temperature range of 1050–1250 °C with the strain rates from 0.01 to 10 s^{-1}. With the increase in deformation temperature and the decrease in strain rate, flow stress of the Ni_3Al-based alloy would be decreased. Based on the obtained constitutive equation, the calculated values of peak flow stress are in good agreement with the experimental ones, and the activation deformation energy is determined as 802.71 kJ/mol. Moreover, by dynamic material model (DMM), processing maps of the hot-deformed Ni_3Al-based alloys are established. It is indicated that the optimum processing parameters for the studied alloy correspond to deformation temperature of 1250 °C and strain rates from 0.01 to 0.1 s^{-1}. Specimens deformed under the optimum processing conditions exhibit fine and uniform grains, which is a typical dynamic recrystallization (DRX) microstructure. The DRX degree could be effectively enhanced with the increase of deformation temperature and the decrease of strain rate.

1. Introduction

Due to the long range ordered structure, the intense action of atomic bonding and the better thermo-physical behavior, intermetallic alloys have been widely used as high temperature structural materials [1–3]. The investigation on intermetallic alloys is generally concentrated on Fe–Al [4], Ti–Al [5,6] and Ni–Al [7] systems. Moreover, Ni_3Al-based alloy has been paid considerable attention owing to its advantages in physical and mechanical properties, such as low density, excellent high-temperature strength and corrosion resistance [7].

Over the past few decades, extensive study on composition optimization, microstructure characteristic, mechanical performance of Ni_3Al based alloys has been performed. Trace boron is added to improve room temperature ductility and grain boundary cohesive strength [8–10]. The addition of chromium is beneficial to reduce environmental embrittlement and oxidation at high temperatures, and molybdenum addition would enhance the solid solution strengthening effect [11,12]. For the deformation behaviors at high temperature, investigations have been conducted on the IC series Ni_3Al-based alloy. Bhattacharya have studied the deformation behavior of IC50 alloy during cold rolling [13]. Prasad have investigated the hot deformation behavior of the as-cast IC396LZr alloy. The kinetic equations and processing maps were obtained. Moreover, dynamic recrystallization takes place at 1250 °C with strain rate of 0.001 s^{-1} [14]. In addition, Wang have studied the hot deformation behavior of Ni_3Al-based alloy MX246A that was developed by Central Iron and Steel Research Institute of China [15]. The JG4246A alloy was developed on the basis of the IC396 series Ni_3Al-based alloy by adjusting the alloying elements of W, Mo, Ti and Hf. In addition, trace Fe is added to improve the weld-ability [16]. However, the hot workability of the JG4246A alloy may be deteriorated or degraded by the addition of the complex alloying elements, which will limit its industrial application. Moreover, as a newly developed Ni_3Al-based alloy, the hot deformation behavior of the JG4246A alloy has not been investigated until now. Therefore, in order to further improve its mechanical performances, more detailed researches should be focused on deformation behavior and hot workability of the JG4246A alloy. In this study, the hot deformation behavior of a Ni_3Al-based alloy under wide range of deformation temperatures and strain rates was explored, aimed at

* Corresponding author.
** Corresponding author.
E-mail addresses: ycliu@tju.edu.cn (Y. Liu), lichongme@tju.edu.cn (C. Li).

http://dx.doi.org/10.1016/j.jallcom.2017.04.116
0925-8388/

clarifying its deformation mechanism and optimizing hot working domains.

2. Experimental procedures

The Ni_3Al-based alloy used in this study was prepared by casting. The chemical composition of the experimental alloy is represented in Table 1. Prior to the hot compression tests, the as-cast ingot was homogenized at 1230 °C for 16 h followed by air cooling to reduce the non-homogeneity in composition and microstructure. Cylindrical specimens with 8 mm diameter and 12 mm height were machined from the homogenized ingot for compression tests. The hot compression tests were carried out on Gleeble-3500 thermo-simulation machine, and the deformed temperatures are ranged from 1050 °C to 1250 °C at an interval of 50 °C with constant strain rates of 0.01, 0.1, 1, 10 s^{-1}. All specimens were heated to the deformation temperature at a rate of 10 °C/s and held for 3 min to obtain homogeneous microstructure, and then compressed to a reduction of 60%. After compression, the specimens were quenched by water immediately to obtain the deformed microstructure. The schematic diagram of the hot compression tests is shown in Fig. 1. In order to minimize the frictions during the hot deformation, the tantalum foils with thickness of 0.1 mm were used between anvils and the specimen surfaces. Hot deformed specimens were sectioned parallel to the compressing direction for the microstructure examination. The mechanical polished specimens were etched for several seconds in a solution of $CrO_3 + HCl + H_2O$. Optical microscope (OM) and scanning electron microscope (SEM) were carried out to investigate the initial and deformed microstructure.

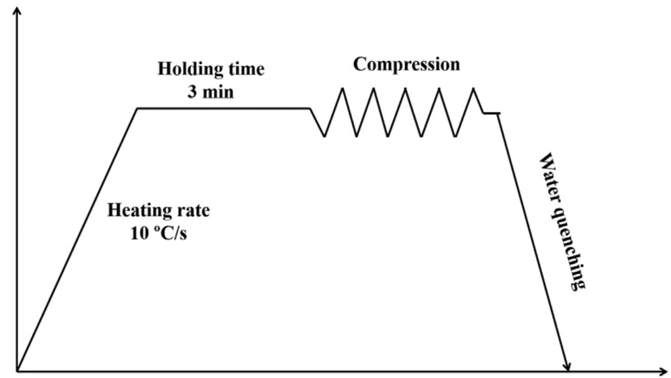

Fig. 1. Schematic diagram of the isothermal compression test.

3. Results and discussion

3.1. Initial microstructure

Fig. 2 shows the initial microstructure of the studied alloy. The average grain size is determined to be about 180 μm by the linear intercept method in three directions [17]. The light areas in Fig. 2(a) represent the dual phase $(\gamma + \gamma')$ structure while the dark areas represent the $\gamma - \gamma'$ eutectic structure. The magnified morphology of the dual phase structure is shown in Fig. 2(b), the regularly packed cuboidal γ' particles with an average size of about 0.5 μm embedded in the γ matrix, and there are some nanometer percipated γ' particles in the γ channels. The energy dispersive spectrometer (EDS) equipped with SEM is applied to reveal the chemical compositions of γ' phases. The EDS result of γ' phase is exhibited in Fig. 3.

3.2. Flow stress behavior

The flow stress curves of the studied alloy at temperature ranging from 1050 to 1250 °C and strain rates from 0.01 to 10 s^{-1} are shown in Fig. 4. It can be found that all of the flow curves exhibit the typical characteristics of DRX [18]. Based on the flow curve of 1100 °C/0.01 s^{-1}, the flow stress is increased rapidly from 0 to 200 MPa at the initial stage of hot deformation, which is due to the dislocation generation and multiplication induced by work hardening [19]. Although the effects of dynamic recovery (DRV) are strengthened with the increase of the applied strain, the work hardening effect can still not be compensated. This results in the continuous increase of flow stress until to the maximum stress, and then DRX occurs. During the DRX process, the flow stress decreases with the strain increasing, since the softening rate caused by DRX and DRV is higher than work hardening rate [20]. Finally, the curve reaches a steady stage owing to the balance between dynamic softening effect and work hardening as the strain reaches 0.8. Moreover, as can be seen from Fig. 4, some flow curves exhibit fluctuation, especially for all the curves at 10 s^{-1}. It could be attributed to an alternation between the work hardening effect and the dynamic softening effect which caused by the rapidly growing grains at high temperature and DRX. Similar phenomenon has also been reported in the IC396LZR alloy [14].

From the curves, it can be found that the applied deformation temperature and strain rate as important processing parameters exert great impact on the flow behavior of this studied alloy. The flow stress decreases with the increase in deformation temperature and the decrease in strain rate, which is typical in most metals and alloys [21–25]. This is because that the dislocation multiplication rate rises with the increase of strain rate at the same deformation temperature, and under the uniform strain rate, the thermal activated DRX can be facilitated with the deformation temperature increasing [26]. Meanwhile, with the decrease in the strain rate or increase in the deformation temperature, the critical strain for DRX is decreased. This could be attributed to the decrease in the critical dislocation density [27].

3.3. Constitutive equation

In order to clarify the relationship between the flow stress, strain rate and deformation temperature, the effective and calculable constitutive equation is adopted. The Arrhenius equation is the most widely accepted, and the type can be expressed as follows [28,29].

$$\dot{\varepsilon} = AF(\sigma)exp\left(-\frac{Q}{RT}\right) \tag{1}$$

where $\dot{\varepsilon}$ is the strain rate (s^{-1}), Q is the activation energy for deformation (J/mol), R is the universal gas constant (8.314 J/mol K),

Table 1
Chemical composition of the experimental JG4246A alloy (wt. %).

C	Cr	Al	Ti	Hf	W	Mo	B	Fe	Si	Mn	Ni
0.06–0.2	7.4–8.2	7.6–8.5	0.6–1.2	0.3–0.9	1.5–2.5	3.5–5.5	<0.05	<2	<0.5	<0.5	Bal.